Thermal Diffusion of C_{60} Molecules and Clusters on Au(111)

Song Guo, Daniel P. Fogarty, Phillip M. Nagel, and S. Alex Kandel*

Department of Chemistry and Biochemistry, University of Notre Dame, Notre Dame, Indiana 46556

Received: April 6, 2004; In Final Form: June 29, 2004

The structure and dynamics of partial monolayers of C_{60} on the Au(111) surface were observed by scanning tunneling microscopy (STM) under ambient conditions. At submonolayer coverages, C_{60} molecules group into islands, and while the molecules in the interior of islands are quite stable, the C_{60}s at island edges are less so, and their motions can be observed in real time using STM. The motion of surface-adsorbed C_{60} is predominantly the result of thermal diffusion; the extent of perturbation by the STM tip is determined to be minimal, using a quantitative analysis of a time series of STM images. Further analysis shows that motion of single C_{60} molecules is relatively uncommon, and that most diffusion of C_{60} on the surface occurs through the correlated or cooperative motion of molecular clusters ranging in size from 2 to 8 C_{60} molecules. Cluster diffusion is explained by a proposed "anchoring" mechanism, in which the stability of each C_{60} varies according to its position and orientation relative to the surface and to neighboring molecules.

Introduction

Fullerenes have attracted tremendous interest since their discovery[1] in 1985, owing to their unique structural, chemical, and electronic properties. There have been efforts devoted to using fullerenes and their derivatives in superconductors, optical devices, microsensors, and electronic devices.[2−7] To pursue these applications, it is important to understand at a fundamental level how fullerene molecules interact physically and electronically with each other and with their local environment. In this manuscript, we present the results of our studies of buckminsterfullerene (C_{60}) molecules adsorbed on gold surfaces. Scanning tunneling microscopy (STM) is used to investigate the structure of C_{60} clusters on gold, as well as to observe thermal diffusion of molecules and clusters on the gold surface. These measurements provide information on how both molecule−molecule and molecule−surface interactions determine the structure and dynamics of surface-adsorbed molecules.

STM, with its ability to image individual molecules, has been widely adopted as a tool to explore fullerene adsorption on surfaces. STM has been used to study C_{60} on a wide range of surfaces of both metallic and semiconducting materials.[8−23] The interaction of C_{60} with a metal substrate is often quite complex, and adsorbate-induced reconstruction of the surface has been reported in a number of instances.[8,20,24] The first STM investigations of C_{60} adsorbed on Au(111) were performed by Altman and Colton,[8−11] who observed two distinct structures for C_{60} monolayers,[8] which were described as having $2\sqrt{3} \times 2\sqrt{3}$ R30° and 38×38 symmetries with respect to the underlying lattice. In a more recent publication, Rogero et al.[25] studied C_{60} monolayers on Au(111) by STM and scanning tunneling spectroscopy (STS). In these experiments, STS measurements suggested a 7×7 overlayer (described by the authors by its 2×2 C_{60} symmetry), with different Au binding sites resulting in observable changes in C_{60} electronic structure. We would suggest that the spectroscopic data strengthen the case for the 7×7 model to be used to describe the structure previously proposed to be a nearly incommensurate 38×38 overlayer, especially as the currently accepted value for the C_{60} nearest-neighbor distance, 10.08 Å, is larger than that used in making the 38×38 assignment, 9.95 Å.

These publications have shown that full C_{60} monolayers are quite stable on the Au(111) substrate. C_{60} intramolecular structure can be imaged, indicating that even rotations of C_{60} on Au(111) are hindered when a full monolayer is formed.[9,25] In contrast, Altman and Colton's results show that individual C_{60} molecules are highly mobile on the gold surface, with single, isolated fullerenes diffusing too quickly to be observed on the time scale of STM imaging. Instead, monolayers nucleate at step edges and grow outward as mobile C_{60} molecules attach themselves.[8]

In general, the relative stability of single-molecule vacancies on Au(111) and Ag(111) suggest that the full, close-packed C_{60} layer is very stable and difficult to reorder.[10] However, in our experiments we observe that submonolayer coverages can result in structures that are fairly stable, and yet show dynamics over long time periods that are readily observed by STM. This behavior was first seen by Altman and Colton,[10] who in one experiment "poked" the STM tip into the surface in order to produce an irregular defect in a C_{60} monolayer. Over the course of about 20 min, several molecules in the created structure were observed to change position, with a trend toward increased coordination with neighboring C_{60} molecules. Other studies have also shown evidence of C_{60} mobility on the surface. Gimzewski et al.[20] acquired time series of STM images for C_{60} on a variety of metal surfaces and showed that on Au(110), reorientation of C_{60} clusters does take place. They additionally showed that the STM tip could be used to manipulate surface C_{60}s under the appropriate STM tunneling conditions, with sufficient precision to create and control molecular structures on the surface.[19−21] Marchenko and Cousty[26] studied the interface between a C_{60}/tetradecane solution and a Au(111) surface by in situ STM. They observed C_{60} islands that exhibited $2\sqrt{3} \times 2\sqrt{3}$ R30° packing symmetry. Some mobility of boundaries of these islands was proposed based on comparison of two consecutive images of the same area.

In this paper, C_{60} is deposited on Au(111) by drop casting fullerenes onto the substrate from a dilute solution. Under our experimental conditions, C_{60} molecules form islands instead of

* E-mail: skandel@nd.edu.

10.1021/jp048481m CCC: $27.50
Published on Web 08/21/2004

full monolayers on the gold surface. The structures created are intermediate between full monolayers and isolated C_{60} molecules, and show interesting dynamical behavior different from that observed at either extreme of coverage. At room temperature, the C_{60} molecules are relatively stable at the centers of those islands, but are mobile at the edges. We are able to show definitively that the observed dynamics are the result of thermal diffusion of C_{60} across the surface. Furthermore, we find that those molecules tend to diffuse on the surface, not through motion of individual molecules, but instead through cooperative or correlated diffusion of midsized clusters. Details of sample preparation and STM measurements will be described in the Experimental section. In the Results section, we will present our main experiment results, concerning the mobility of C_{60} molecules on Au(111) by STM at room temperature under ambient conditions. In the Discussion section, we will discuss those results based on consideration of both adsorbate−substrate and adsorbate−adsorbate interactions.

Experimental Section

Apparatus. All experiments were performed with a home-built scanning tunneling microscope (STM) operated at room temperature under ambient (atmospheric) conditions. The microscope is based on a PZT tube scanner (Staveley Sensors Inc., EBL-1) and uses a one-dimensional inertial slider (Omicron Instruments, MS-5) for coarse sample approach. STM tips for this study were mechanically clipped sections of 0.25-mm Pt-Ir(80:20) wire. Electronics from RHK Technology were used for microscope control and data acquisition.

All images presented were acquired in constant-current mode, with a sample bias voltage of 0.15 V and a tunneling current of 40 pA. This tunneling current is substantially smaller than operating currents reported in previous studies, and normally a higher tunneling current is required to observe the intramolecular structure of C_{60} molecules. Here we use this relatively low current to avoid the possibility of tip-induced motions of C_{60} molecules, which will be discussed in the following sections. Most images presented here show raw, unfiltered data; Figure 2 is presented after Fourier filtering to remove high-frequency noise.

Sample Preparation. The C_{60} (99.9+%) is purchased from Alfa Aesar and used "as is". A dilute solution of C_{60} in either dichloromethane or benzene is formed by dissolving 0.5 mg of the fullerene powder in 10 mL of solvent. The solution is used almost immediately, before solvation is complete, and so the actual concentration is substantially more dilute. This allows us to avoid the use of heat, sonication, or excessive solvation time, all of which could possibly result in reaction and degradation of the C_{60}. The Au(111)-on-mica substrate is purchased from Molecular Imaging and gently annealed in a hydrogen flame prior to use. Before depositing C_{60} on the surface, we use STM to image the surface, to make sure the surface is clean and crystalline. After flame annealing, we observe large, clean terraces with occasional single-atom-deep "pits" approximately 25−75 Å in diameter. After verifying the cleanliness of the gold substrate, one or two drops of freshly made C_{60} solution are added to the surface, and the solvent is allowed to evaporate. After imaging is done, the gold sample is discarded, as we are not certain that fullerenes can be completely removed from the surface in a reliable fashion. The drop-casting method does not afford precise control of the surface coverage, but most of our samples were produced with coverages less than a full monolayer.

Published reports indicate that C_{60} is likely to degrade in the presence of either ultraviolet light or atmospheric ozone.[27−30] To alleviate this concern, we tested samples that were several days old, and observed that the appearance of C_{60} molecules and islands in STM images was relatively unchanged. Nevertheless, all the data presented in this paper were taken within five hours of the drop-casting time.

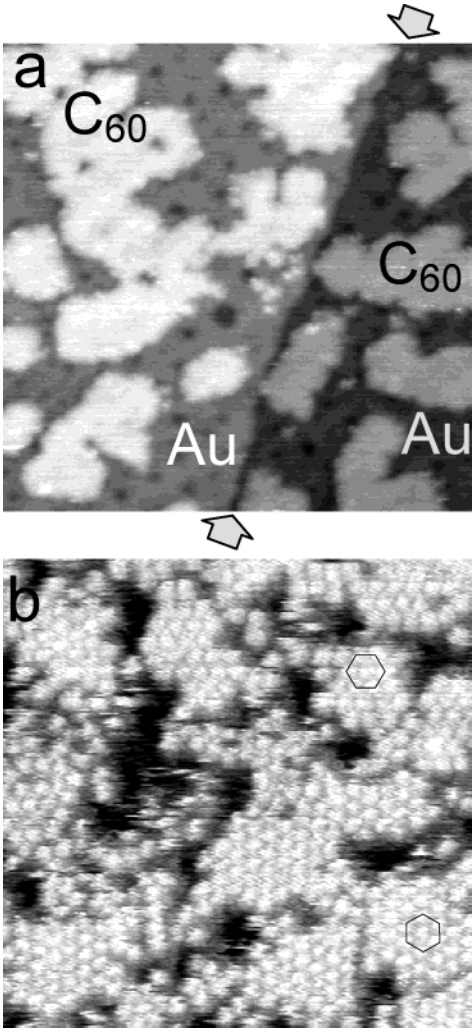

Figure 1. (a) Constant-current STM image of a partial C_{60} monolayer on Au(111); image size is 1150 Å × 1150 Å. Two atomic terraces are shown, with the lower terrace on the right-hand side of the image; the step (indicated by arrows) cuts diagonally down the image from the upper right-hand corner. C_{60} islands of various shapes and sizes appear on both terraces 4.0 Å higher than the bare gold substrate. Dark features visible on the upper terrace result from gold-atom vacancies. (b) A 270 Å × 270 Å molecular-resolution image showing small, close-packed C_{60} islands in two distinct rotational domains (indicated by two hexagons drawn over the image). Disordered regions are also visible.

Results

A representative image of a partial C_{60} monolayer is shown in Figure 1a. Single-molecule-high "islands" (4.0 Å apparent topographic height) of C_{60} are observed, and vary in size from 100 to 400 Å. Island size and surface coverage depend on the specifics of surface preparation; in all cases, however, the types of structures formed are significantly different from those observed by Altman and Colton.[8] Altman and Colton have reported that single C_{60} molecules diffuse very quickly on the Au(111) surface at room temperature, with monolayer nucleation beginning at step edges.[8] In our experimental conditions, after drop-casting the C_{60} molecules on Au(111), C_{60} islands are distributed randomly on the surface. No clear preference for

nucleation at step edges is observed. Given the high density of Au vacancy defects (dark features on the bare gold terraces) on the surface, the possibility of nucleation at these defects cannot be ruled out. However, these observations suggest that the mechanism for island growth is potentially different from that observed in the Altman and Colton studies (although, in contrast, island nucleation on terraces is observed by Gimzewski et al.[20] on (110) metal surfaces). This result is not surprising, as the kinetics of deposition from solution are quite likely to be very different from those for deposition in vacuum.[31,32]

Figure 1b presents a higher-resolution STM image that shows that C_{60} adopts a hexagonally close-packed structure on the surface, as reported previously.[8] The surface shown in Figure 1b is covered mostly by small, well-ordered, close-packed C_{60} islands; however, disordered C_{60} molecules can also be observed.

As we discussed previously, there are two C_{60} hexagonal surface structures commensurate with the Au(111) lattice that result from vacuum deposition: $2\sqrt{3} \times 2\sqrt{3}\,\mathrm{R30°}$ and 7×7.[8,25] Both C_{60} structures result from solution-phase deposition. We do not make these assignments directly, as the STM cannot resolve Au atomic structure with the mild tunneling conditions used to image C_{60} molecules; however, strong indirect evidence is available. The image shown in Figure 1b contains small C_{60} domains in only two distinct rotational orientations, with close-packed directions 30° apart (indicated on the figure by the two overlaid hexagons). In other images, we have been able to compare the lattice orientation of C_{60} islands to the directions of gold step edges (which typically align along Au lattice directions for Au(111)).

Some of the features in the image shown in Figure 1b exhibit streakiness, which is due to diffusion of C_{60} on the time scale of the STM fast-scan rate.[33] We observe this fast diffusion predominantly for C_{60} molecules isolated on bare gold terraces, as well as for small, disordered C_{60} islands; this is in agreement with earlier observations indicating free motion of single C_{60} molecules on the surface.[8]

In contrast to the fast diffusion of isolated molecules, C_{60} molecules associated with an ordered, close-packed island are far more stable, and diffuse on a much longer time scale. The mobility of C_{60} islands in our experiments is shown in Figure 2. Figure 2 presents three topographic images taken in the same area, from a series of images taken over 15 min. These images are cropped from the raw data to show the exact same area after accounting for the thermal drift (which has the effect of moving the scan window roughly 10 Å between images). The C_{60} molecules in the middle of close-packed islands were very stable and showed little change. However, at the island edges, molecules have the freedom to move around, and small but distinct structural changes are observed when comparing these three images.

In any STM measurement of dynamic processes on surfaces, it is critically important to rule out perturbation of the sample by the STM tip (so-called "tip-induced motion"). In STM measurements, the tunneling conditions determine the interactions between tip and sample, and thus must be chosen carefully. Decreasing the tunneling current will lead to a larger tip−sample distance, attenuating any van der Waals interaction between the tip and the sample. Lowering the bias voltage, on the other hand, can decrease the electric field at the surface and therefore limit field-induced surface changes (though lower bias voltages can also result in smaller tip−sample separations). Previous studies have largely focused on maximizing image resolution for C_{60} on gold, with tunneling currents ranging from 0.1 to 1.0 nA, and voltages from 0.5 to 3.0 V reported in the literature.[8,25] In the current study, we attempted to minimize tip-induced motion by using substantially milder tunneling conditions: 0.15 V bias and 40 pA tunneling current. Using these conditions, image features that are qualitatively associated with tip-induced motion are almost completely eliminated. Specifically, streaking in the STM fast-scanning direction is not observed for ordered C_{60} islands (but can still be seen for isolated, disordered C_{60}s, as in Figure 1b).

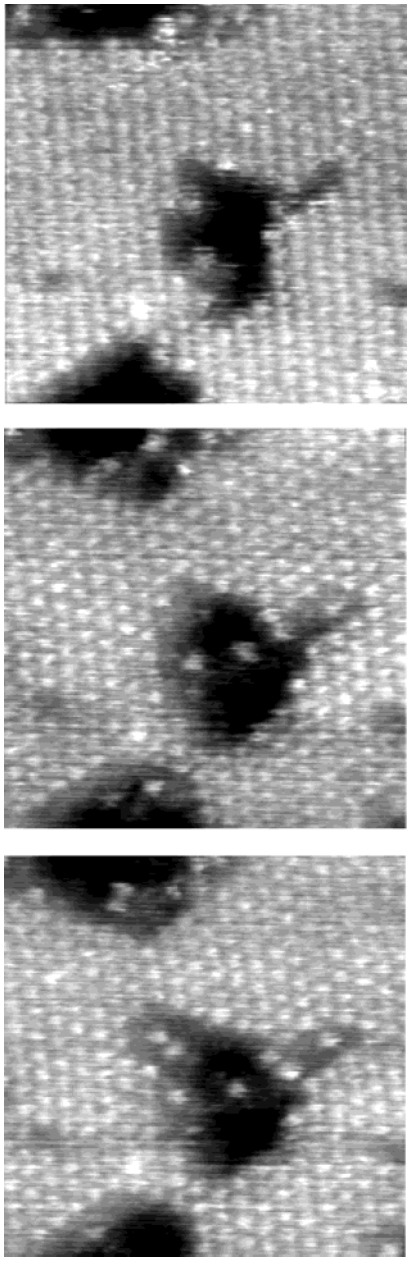

Figure 2. Three molecular-resolution STM images of a partial C_{60} monolayer on Au(111) from a 15-min series of images, 200 × 200 Å. In general, C_{60} molecules in the middle of close-packed islands are very stable, while molecules at the island edges show higher mobility. Structural changes are observed on the minute time scale, as molecules rearrange near defects and island edges.

To rule out quantitatively the possibility of significant tip-induced motion, we acquired a series of STM images of the same area and systematically varied the elapsed time between image acquisitions. In this fashion, the effects of thermal diffusion (which should depend only on the elapsed time between images) and tip-induced motion (which should increase as the tip is scanned more frequently across the surface) can be separated.

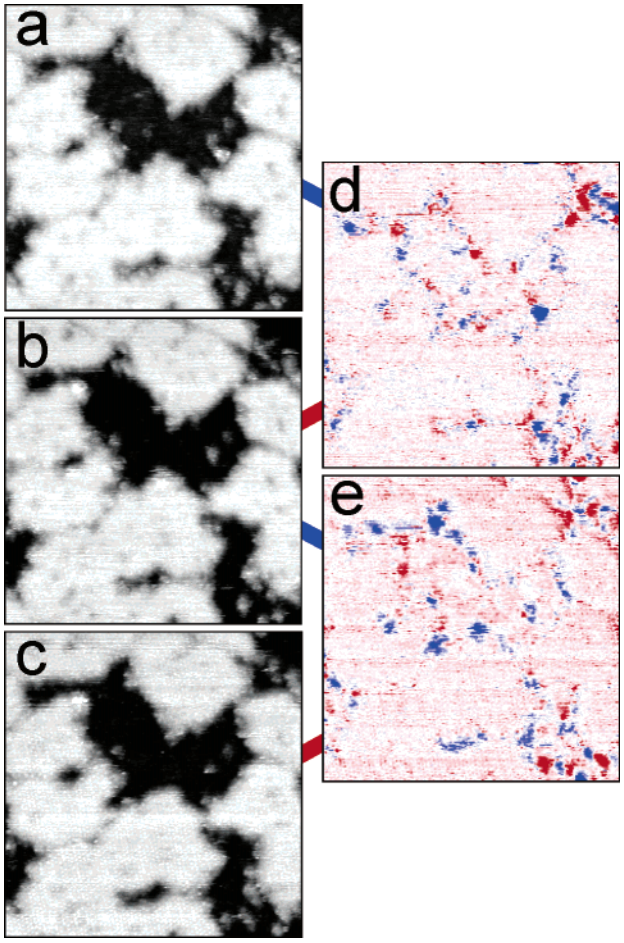

Figure 3. (a)−(c) Three STM images, 770 × 770 Å, consecutively acquired over the same area of the surface. A total of 8 min elapsed between images (a) and (b), and 7.5 min between images (b) and (c). Three additional images (not shown here) were recorded between image (b) and image (c) to demonstrate that increased scanning does not result in greater changes in the image. Panel (d) shows the numerical difference obtained by subtracting the data in image (b) from that of (a); panel (e) is from subtracting (c) from (b). These numerically differenced composite images are shown with a red-white-blue diverging color scheme, so that blue features indicate C_{60} molecules present in the first image but absent in the second one. Conversely, red features show C_{60} molecules absent in the first image but present in the second one.

In Figure 3, panels a−c present three images taken from a series of six. The elapsed time between images (a) and (b) is approximately eight minutes; images (b) and (c) are similarly spaced, by approximately eight minutes in time. However, there were three additional images (not shown here) recorded between image (b) and image (c). In contrast, (b) was acquired immediately following (a). Thus, if tip-induced perturbations are significant in these images, we would expect substantially greater differences between images (b) and (c) than between (a) and (b). We will show with the following analysis that this is not the case, and that tip-induced perturbations do not play a major role in C_{60} diffusion.

After correcting for thermal drift, differences between these images are evident, though quite small. To highlight the differences between images, we numerically subtracted the data in image 3b from that in 3a (after correcting for the effect of thermal drift and piezoelectric "creep") to produce the composite image shown as Figure 3d. Figure 3e was obtained in the same manner by numerically subtracting 3c from 3b. These composite images are presented with a red-white-blue diverging color scheme; areas that are unchanged between the original images appear in white. Blue features in the composite images result from C_{60} molecules present in the first image and absent in the second one; similarly, red features indicate C_{60} molecules absent in the first image but present in the second one.

By comparing the composite images shown in panels 3d and 3e, we draw the conclusion that observed changes are largely the result of thermal motion, and that tip-induced motion plays at most a minor role. If, contrary to this conclusion, the motions of C_{60} on the surface were mainly tip-induced, the differences between images 3b and 3c should be almost three times bigger than those between images 3a and 3b. The similarity in the number of red and blue features in the two composite images demonstrates that this is not the case. The images in Figures 3d and 3e are instead qualitatively similar, and thus the diffusion of C_{60} molecules on the surface is largely unaffected by the number of intervening scans. This indicates that thermal motion of C_{60} molecules plays the dominant role in our experiments. We have performed a number of similar measurements, with results reproducing those shown here; quantitative analysis of these images supports our conclusion, and will be discussed presently.

We have no evidence that suggests that there is any solvent remaining on the surface, and we do not believe that the C_{60} diffusion is influenced by residual solvent. We obtain identical results regardless of whether the surface is prepared through drop casting from dichloromethane or benzene solution. Additionally, the behavior we observe is quite similar to that reported by Altman and Colton[10] for rearrangement of a tip-induced defect in a C_{60} monolayer in vacuum.

After comparing the composite images in Figure 3d and 3e (which show molecular motion) with the images in Figure 3a−c (which largely show static structure), we see that the great majority of molecular diffusion events occur either at the edges of C_{60} islands or in very small, isolated clusters. Island edges are intermediate between full monolayers and single surface-bound molecules, so it is reasonable that they show neither complete stability nor fast diffusion. Diffusion of molecules at island edges is, indeed, exceptionally slow, with only a small fraction of C_{60} molecules changing position over a period of several minutes.

The red and blue features in Figures 3d and 3e are significantly larger than single C_{60} molecules. Through analysis of these images, we observe that diffusion of C_{60} on Au(111) occurs mainly by the motion of molecular clusters. This is further borne out by the observation that many features in these composite images are "paired", with a red feature near a blue feature of similar size and shape. These large, paired features result from clusters of C_{60} molecules moving from one location to another. In some cases, these paired features do not have the same shape, indicating rearrangements of C_{60} molecules during the diffusion process.

The scale of the images shown in Figure 3 makes it difficult to determine exact cluster size by counting individual C_{60} molecules. Instead, we estimate the number of molecules in each cluster from the cluster area. Red and blue features corresponding to clusters were identified in the images and analyzed using feature detection and analysis routines (MatLab 6.5, The MathWorks Inc.). In total, we analyzed 15 images, measuring 439 clusters. The resulting data are shown in a "skyscraper" plot in Figure 4. These data should be viewed qualitatively, as there are three factors that could lead to errors in cluster size determination: (1) single-molecule diffusion events are harder to identify than diffusion of large clusters, likely leading to

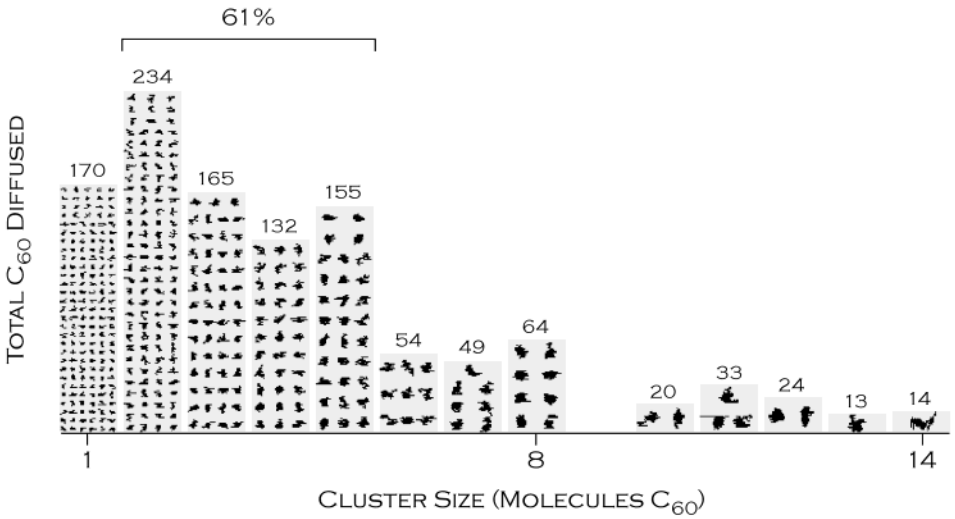

Figure 4. "Skyscraper" plot, showing the size distribution of diffusing C_{60} clusters. There were 15 images analyzed, yielding 439 cluster diffusion events. The diffusing clusters are grouped by size (in number of molecules, from 1 to 14) to make a histogram. The height of each light gray histogram bar is set so that the area of the bar is proportional to the number of molecules diffusing; this total is posted above each bar. Superimposed on each histogram bar are the raw, unfiltered data for each cluster measured. 61% of C_{60}s that are observed to diffuse do so as members of clusters containing 2 to 5 molecules.

undercounting of one- and two-molecule clusters; (2) two or more clusters that diffuse to or from the same location will be counted by the software as a single, larger cluster; and (3) instrumental noise in the images causes some variation in cluster area, and can additionally cause larger clusters to appear broken up into two or more smaller clusters. The data for all observed clusters are superimposed on the histogram bars to allow these effects to be assessed by the reader; while there is some noise, the shapes of the clusters are well determined and independent of the scan direction (which is vertical for the 14-molecule cluster, and horizontal for all other images recorded). From these data (and from the difference images in Figures 3d and 3e), it is clear that cluster diffusion plays the dominant role in C_{60} mobility on the surface; 61% of C_{60} molecules that are observed to diffuse on the surface do so as part of a two- to five-molecule cluster.

The above analysis was also used to determine the total number of C_{60} molecules diffusing between each pair of images. These data allow a quantitative determination of the relative importance of thermal diffusion and tip-induced motion for C_{60} on Au(111). We found that for pairs of images 8 min apart, 21.2 ± 2.9 molecules diffused per μm^2 imaged per second. When we increased the scanning rate so that five images were acquired in the same time period, the rate of observed diffusion is statistically unchanged: 24.6 ± 6.7 molecules diffused per μm^2 imaged per second.

The similarity of these numbers shows that STM scanning has little or no effect on our images, and that the observed changes must be due to thermal diffusion of C_{60} molecules and clusters. We have performed preliminary experiments to further explore this thermal diffusion process, in which the sample temperature was varied over a range of 10 °C. First results indicate that even these modest temperature changes produce an observable difference in diffusion rates, and these experiments will be detailed extensively in a future publication.

Discussion

We have measured partial C_{60} monolayers on Au(111) using STM under ambient conditions. "Drop casting" the C_{60} onto the surface from solution results in the formation of close-packed molecular islands; This coverage regime is intermediate between isolated, surface-adsorbed molecules and a full molecular monolayer. At room temperature, C_{60} islands show most of the stability previously reported for full monolayers, but we find that molecules bound at island edges and near defects exhibit observable but extremely slow diffusion. An analysis of the STM data demonstrates that diffusion is due to thermal effects, and the possibility of substantial perturbation by the STM tip is quantitatively excluded.

One of the most interesting results in this study is the observation of significant diffusion of small molecular clusters: over 80% of C_{60}s that diffuse on the Au(111) surface do so as part of clusters. Observations of cooperative diffusion of nanoscale clusters on surfaces have been reported previously for a number of systems.[34−40] In all of these cases, collective diffusion has been observed (experimentally and theoretically) for isolated clusters on surfaces. These observations are usually described in terms of slip-diffusion processes, where clusters first lose registry with the corrugation of the underlying substrate, and can then diffuse freely across the surface. While such a model could provide a mechanism for how small C_{60} clusters diffuse across the Au(111) surface, it is unable to explain how C_{60} clusters break off from C_{60} islands, as this initial step of the diffusion process necessarily requires disruption of more nearest-neighbor interactions than does the departure of a single molecule. In this section, we suggest a possible model for C_{60} cluster diffusion based upon molecule-to-molecule variations of the C_{60}/C_{60} and C_{60}/Au interactions.

For diffusion on the surface, the strength of the C_{60}/Au interaction (approximately 2.2−2.6 eV[8−10]) is relatively unimportant compared to the corrugation energy as the C_{60} molecule interacts with different surface binding sites, such as top, bridge, or hollow sites. The C_{60}/Au interaction will additionally depend on the C_{60} orientation. C_{60} on Au(111) is orientationally locked, with several static molecular orientations observed via STM at room temperature.[8,10,25] The formation of commensurate monolayers from molecules in fixed orientations suggests that the binding energy of C_{60} on Au(111) depends strongly on the molecular position as well. While the adsorption of C_{60} on Au(111) has not been studied theoretically in great detail, ab initio calculations by Ogawa et al.[41] for C_{60} on Cu(111) show that the adsorption energy depends significantly on both the

C_{60} orientation and the Cu binding site; C_{60} molecules adsorbed on Cu(111) have up to a 0.5 eV variation in adsorption energy with orientation, compared with a total heat of adsorption ranging from 2.4 to 3.0 eV. Although the interactions of C_{60} with Au(111) and Cu(111) will not be identical, it is reasonable to believe that sizable orientation effects will exist on Au(111) as well.

The C_{60}/C_{60} interaction has been characterized theoretically as a van der Waals-like potential, and the intermolecular interaction energy thus will depend on the number, distance, and position of neighboring C_{60} molecules.[42−46] Greater numbers of neighboring C_{60} molecules will increase the total interaction energy, thus helping to stabilize the C_{60} layer. This explains why C_{60} molecules in the center of monolayer islands are very stable, while a single adsorbed C_{60} molecule on the surface can show very high mobility;[8] this additionally explains why we see slow diffusion rates at monolayer island edges. It is important to note, however, that the C_{60}/C_{60} interaction is not isotropic, and the interaction energy of two C_{60} molecules has been calculated to depend on their relative orientation by as much as 140−240 meV.[47] This is supported experimentally by the existence of an orientational order−disorder transition at 249 K for bulk face-centered-cubic solid C_{60}.[48]

The extremely slow rate of diffusion observed indicates that we are operating at the very tail of the distribution for thermally activated processes. Thus, molecular motion will be initiated only by the molecule most weakly bound to the island edge. In our proposed model of C_{60} surface diffusion, we refer to this molecule as the "anchor", as once it leaves the edge, all of its former neighbors become destabilized. Indeed, the variation of energies due to molecular orientation and position means that one or more of these neighbors will then likely be bound with less energy than that initially required to remove the anchor. These neighbors will then diffuse exponentially faster, and the diffusion of the anchoring molecule thus acts as the rate-limiting step for the motion of several surface-bound C_{60}s. The overall process consists of correlated molecular motion, and will be observed (at the time scales of STM imaging) as cluster diffusion.

If each C_{60} were bound to its neighbors and to the surface through identical, isotropic interactions, diffusion would be molecular in nature; once one C_{60} moves from its initial position, the ones nearby would be no more likely to diffuse than those molecules further away. Hence, molecule-to-molecule variation of binding energies is essential to explain cluster diffusion. Variations in binding energy will result from differing C_{60}/C_{60} and C_{60}/Au interactions, but the relative importance of these interactions will depend on whether the C_{60} monolayer assumes a 7×7 or a $2\sqrt{3} \times 2\sqrt{3}$ R30° structure. Schematics of both of these monolayer structures are shown in Figure 5.

The unit cell of the 7×7 structure is two C_{60}s long per side, and contains one molecule bound at an atop site and three at bridge sites. As we discussed previously, theoretical simulations of C_{60} on Cu(111) show variations in binding energy with adsorption sites of up to 0.5 eV.[41] For C_{60} on Au(111), Rogero et al.[25] performed scanning tunneling spectroscopy (STS) measurements of the molecules in the 7×7 structure and showed that the degree of electron transfer between C_{60} and the surface was adsorption-site-dependent. A DFT analysis of these results by Pérez-Jiménez et al.[49] suggests that binding is favored at bridge sites, with the energy difference for bridge versus atop adsorption possibly as large as 0.82 eV. This contradicts earlier experimental work by Altman and Colton,[9] which showed atop adsorption was preferred. Despite conflicts in the literature, it is a certainty that the different adsorption sites in the 7×7 structure will lead to considerable variations in C_{60} binding energy.

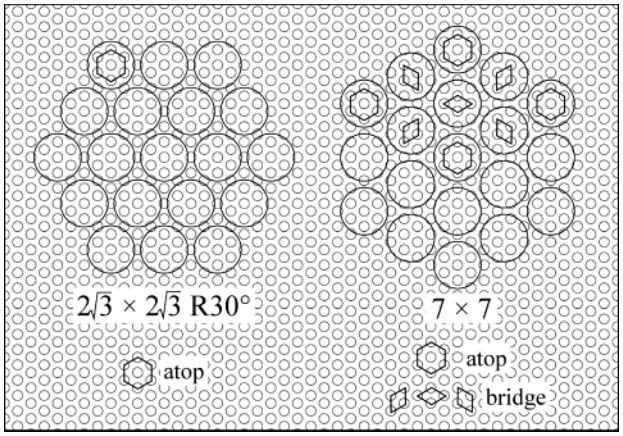

Figure 5. Diagram showing the 7×7 and $2\sqrt{3} \times 2\sqrt{3}$ R30° structures for C_{60} monolayers on Au(111). In the $2\sqrt{3} \times 2\sqrt{3}$ R30° structure, every C_{60} molecule is at an atop position; in the 7×7 structure, there are inequivalent sites for C_{60} molecules: atop or bridge. The $C_{60}-C_{60}$ distances for ideal 7×7 and $2\sqrt{3} \times 2\sqrt{3}$ R30° structures are 10.08 and 9.98 Å, respectively.

For the purpose of example, we assume for the moment that the atop site is preferred for binding (in keeping with the Altman and Colton conclusions[9]) for the hexagonal cluster shown in Figure 5. Each corner molecule of this cluster then acts as an "anchor", stabilized by the C_{60}/Au interaction. Once a corner molecule diffuses, however, its three former neighbors will all be at bridge sites, will consequently be less stably bound, and will leave the cluster at a far greater rate. This example may also provide insight into the observed size distribution for cluster diffusion; diffusing clusters are predominantly 2 to 5 C_{60}s in size, in agreement with the four-molecule unit cell of the 7×7 structure.

The overall concepts of the anchoring model can still apply even if, instead, bridge-site binding is preferred over atop (in accordance with the DFT calculations of Pérez-Jiménez et al.[49]) In this case, it is corner molecules at bridge sites that will act as anchors, and more weakly bound molecules at atop sites that will subsequently diffuse after the anchor has left. The overall behavior will be very similar: the variation of binding energies in the 7×7 structure will cause significant dispersion in diffusion rates that, on the slow time scale of STM imaging, will be seen as cluster diffusion. Further experimental and theoretical investigations of the nature and relative stability of the different binding geometries would be invaluable for quantitative modeling of the cluster diffusion mechanism.

For the perfect $2\sqrt{3} \times 2\sqrt{3}$ R30° monolayer structure, all molecules are at equivalent adsorption sites. Near the edges of molecular islands, this structure could relax or reconstruct, but as this is not evident in our STM images or in the literature, this effect is probably minimal. Any significant variation in C_{60} binding energy can thus only result from the effects of molecular orientation. As described above, both the C_{60}/C_{60} and C_{60}/Au interactions are significantly anisotropic; STM measurements have resolved intramolecular structure, indicating that each molecule is orientationally locked, though long-range orientational order has not been reported.[9,25] We expect that the $2\sqrt{3} \times 2\sqrt{3}$ R30° structure will exhibit slower diffusion than the 7×7 (as it is the more stable structure), but also that cluster

diffusion will be less prevalent. Experiments to probe the effect of the overlayer structure on the diffusion process are currently underway.

The time scale for cluster diffusion in the C_{60}/Au(111) system is exceptionally slow; diffusion occurs not over a few picoseconds or milliseconds[50,51] but over minutes and hours. These dynamics are typical for a glassy system, and there are several reasons to believe that surface-adsorbed C_{60} has glasslike characteristics. While STM images have shown that C_{60} is rotationally locked on Au(111), no long-range orientational order has been reported. Furthermore, the coexistence of two distinct monolayer structures on the surfaces demonstrates that the system is not at a thermodynamic minimum, but is instead in a kinetically trapped structure. This is unsurprising, as sample preparation by drop casting can easily result in nonequilibrium surface structures.[31,32,34] Finally, our preliminary studies of the temperature dependence of diffusion indicate sizable changes in diffusion rates over a fairly small range of temperatures.

There are notable similarities between surface-adsorbed C_{60} on Au(111) and the glassy systems modeled theoretically by Glotzer and co-workers.[52−55] In a recent paper, Gebremichael et al.[52] reported results of molecular dynamics simulations showing correlated motion in a single-component glass. In this system, interactions between atoms were described by a Dzugotov potential. This potential approximates a Lennard-Jones potential at short range, but is modified by the addition of a potential maximum at intermediate distances. This second maximum allows for glass formation, and results in dynamics that include multiple-atom correlated-motion events, in which one-dimensional "chains" of atoms diffuse together. The physical processes underlying C_{60}/C_{60} interactions on Au(111) are clearly very different from those modeled in the Dzugotov potential (which is used to approximate metal/metal interactions); we propose, however, that the functional form is distinctly similar. The C_{60}/C_{60} interaction is van der Waals in nature; however, the interaction energy between any two neighboring molecules will also depend on their positions with respect to the gold lattice. The combination of the C_{60}/C_{60} interaction with the C_{60}/Au interaction will likely result in additional maxima and minima in the potential. This will be most pronounced in the 7×7 structure, where molecules are bound at nonequivalent surface sites. Conversely, we would predict that $2\sqrt{3} \times 2\sqrt{3}$ R30° islands would, in the absence of strong orientational effects, show little diffusion.

Solution-phase deposition of C_{60} onto Au(111) results in partial monolayer coverages, with molecules at the edges of monolayer islands exhibiting long time-scale diffusion, predominantly in the form of molecular clusters. We have suggested an anchoring model that explains cluster diffusion in terms of correlated molecular motion that results from molecule-to-molecule variations in C_{60}/Au and C_{60}/C_{60} binding energies. This model differs substantially from the slip-diffusion mechanisms commonly used to explain cooperative motion of molecules or nanoparticles; however, there are some conceptual similarities to the chainlike diffusion seen in glassy systems. We are currently exploring the effect of molecular-scale structure of island edges on cluster diffusion rates as a means of refining the models presented in this study.

Acknowledgment. This work was supported by the Petroleum Research Fund, Grant #38101-G5. The authors thank Prof. J. Daniel Gezelter for helpful discussions.

References and Notes

(1) Kroto, H. W.; Heath, J. R.; Obrien, S. C.; Curl, R. F.; Smalley, R. E. *Nature* **1985**, *318*, 162.
(2) Haddon, R. C.; Perel, A. S.; Morris, R. C.; Palstra, T. T. M.; Hebard, A. F.; Fleming, R. M. *Appl. Phys. Lett.* **1995**, *67*, 121.
(3) Sun, Y. P.; Riggs, J. E. *Int. Rev. Phys. Chem.* **1999**, *18*, 43.
(4) Sherigara, B. S.; Kutner, W.; D'Souza, F. *Electroanalysis* **2003**, *15*, 753.
(5) Forro, L.; Mihaly, L. *Rep. Prog. Phys.* **2001**, *64*, 649.
(6) Shinohara, H. *Rep. Prog. Phys.* **2000**, *63*, 843.
(7) Kelly, K. F.; Sarkar, D.; Hale, G. D.; Oldenburg, S. J.; Halas, N. J. *Science* **1996**, *273*, 1371.
(8) Altman, E. I.; Colton, R. J. *Surf. Sci.* **1992**, *279*, 49.
(9) Altman, E. I.; Colton, R. J. *Phys. Rev. B* **1993**, *48*, 18244.
(10) Altman, E. I.; Colton, R. J. *Surf. Sci.* **1993**, *295*, 13.
(11) Altman, E. I.; Colton, R. J. *J. Vac. Sci. Technol., B* **1994**, *12*, 1906.
(12) Pedersen, M. O.; Murray, P. W.; Laegsgaard, E.; Stensgaard, I.; Besenbacher, F. *Surf. Sci.* **1997**, *389*, 300.
(13) Murray, P. W.; Pedersen, M. O.; Laegsgaard, E.; Stensgaard, I.; Besenbacher, F. *Phys. Rev. B* **1997**, *55*, 9360.
(14) Johansson, M. K. J.; Maxwell, A. J.; Gray, S. M.; Bruhwiler, P. A.; Mancini, D. C.; Johansson, L. S. O.; Martensson, N. *Phys. Rev. B* **1996**, *54*, 13472.
(15) Maxwell, A. J.; Bruhwiler, P. A.; Arvanitis, D.; Hasselstrom, J.; Johansson, M. K. J.; Martensson, N. *Phys. Rev. B* **1998**, *57*, 7312.
(16) Zhang, Y.; Gao, X. P.; Weaver, M. J. *J. Phys. Chem.* **1992**, *96*, 510.
(17) Lu, X. H.; Grobis, M.; Khoo, K. H.; Louie, S. G.; Crommie, M. F. *Phys. Rev. Lett.* **2003**, *90*, 096802.
(18) Yuan, L. F.; Yang, J. L.; Wang, H. Q.; Zeng, C. G.; Li, Q. X.; Wang, B.; Hou, J. G.; Zhu, Q. S.; Chen, D. M. *J. Am. Chem. Soc.* **2003**, *125*, 169.
(19) Cuberes, M. T.; Schlittler, R. R.; Gimzewski, J. K. *Appl. Phys. A* **1998**, *66*, S669.
(20) Gimzewski, J. K.; Modesti, S.; David, T.; Schlittler, R. R. *J. Vac. Sci. Technol., B* **1994**, *12*, 1942.
(21) Cuberes, M. T.; Schlittler, R. R.; Gimzewski, J. K. *Appl. Phys. Lett.* **1996**, *69*, 3016.
(22) Sakurai, T.; Wang, X. D.; Xue, Q. K.; Hasegawa, Y.; Hashizume, T.; Shinohara, H. *Prog. Surf. Sci.* **1996**, *51*, 263.
(23) Mirkin, C. A.; Caldwell, W. B. *Tetrahedron* **1996**, *52*, 5113.
(24) Wang, H. Q.; Hou, J. G.; Takeuchi, O.; Fujisuku, Y.; Kawazu, A. *Phys. Rev. B* **2000**, *61*, 2199.
(25) Rogero, C.; Pascual, J. I.; Gomez-Herrero, J.; Baro, A. M. *J. Chem. Phys.* **2002**, *116*, 832.
(26) Marchenko, A.; Cousty, J. *Surf. Sci.* **2002**, *513*, 233.
(27) Akselrod, L.; Byrne, H. J.; Thomsen, C.; Mittelbach, A.; Roth, S. *Chem. Phys. Lett.* **1993**, *212*, 384.
(28) Juha, L.; Krasa, J.; Laska, L.; Hamplova, V.; Soukup, L.; Engst, P.; Kubat, P. *Appl. Phys. B* **1993**, *57*, 83.
(29) Chibante, L. P. F.; Heymann, D. *Geochim. Cosmochim. Acta* **1993**, *57*, 1879.
(30) Taylor, R.; Parsons, J. P.; Avent, A. G.; Rannard, S. P.; Dennis, T. J.; Hare, J. P.; Kroto, H. W.; Walton, D. R. M. *Nature* **1991**, *351*, 277.
(31) Rabani, E.; Reichman, D. R.; Geissler, P. L.; Brus, L. E. *Nature* **2003**, *426*, 271.
(32) Tang, J.; Ge, G. L.; Brus, L. E. *J. Phys. Chem. B* **2002**, *106*, 5653.
(33) Kushmerick, J. G.; Weiss, P. S. *J. Phys. Chem. B* **1998**, *102*, 10094.
(34) Ge, G. L.; Brus, L. E. *Nano Lett.* **2001**, *1*, 219.
(35) Mitsui, T.; Rose, M. K.; Fomin, E.; Ogletree, D. F.; Salmeron, M. *Science* **2002**, *297*, 1850.
(36) Kurpick, U.; Fricke, B.; Ehrlich, G. *Surf. Sci.* **2000**, *470*, L45.
(37) Kyuno, K.; Ehrlich, G. *Phys. Rev. Lett.* **2000**, *84*, 2658.
(38) Morgenstern, K.; Rosenfeld, G.; Laegsgaard, E.; Besenbacher, F.; Comsa, G. *Phys. Rev. Lett.* **1998**, *80*, 556.
(39) Wang, S. C.; Kurpick, U.; Ehrlich, G. *Phys. Rev. Lett.* **1998**, *81*, 4923.
(40) Luedtke, W. D.; Landman, U. *Phys. Rev. Lett.* **1999**, *82*, 3835.
(41) Ogawa, A.; Tachibana, M.; Kondo, M.; Yoshizawa, K.; Fujimoto, H.; Hoffmann, R. *J. Phys. Chem. B* **2003**, *107*, 12672.
(42) Saito, S.; Oshiyama, A. *Phys. Rev. Lett.* **1991**, *66*, 2637.
(43) Girifalco, L. A. *J. Phys. Chem.* **1991**, *95*, 5370.
(44) Wales, D. J. *J. Chem. Soc., Faraday Trans.* **1994**, *90*, 1061.
(45) Hasegawa, M.; Nishidate, K.; Katayama, M.; Inaoka, T. *J. Chem. Phys.* **2003**, *119*, 1386.
(46) Girifalco, L. A.; Hodak, M.; Lee, R. S. *Phys. Rev. B* **2000**, *62*, 13104.
(47) Larocca, G. C. *Europhys. Lett.* **1994**, *25*, 5.
(48) Heiney, P. A.; Fischer, J. E.; McGhie, A. R.; Romanow, W. J.; Denenstein, A. M.; McCauley, J. P.; Smith, A. B.; Cox, D. E. *Phys. Rev. Lett.* **1991**, *66*, 2911.
(49) Perez-Jimenez, A. J.; Palacios, J. J.; Louis, E.; Sanfabian, E.; Verges, J. A. *ChemPhysChem* **2003**, *4*, 388.

(50) Landman, U.; Luedtke, W. D.; Burnham, N. A.; Colton, R. J. *Science* **1990**, *248*, 454.
(51) Joyce, S. A.; Thomas, R. C.; Houston, J. E.; Michalske, T. A.; Crooks, R. M. *Phys. Rev. Lett.* **1992**, *68*, 2790.
(52) Gebremichael, Y.; Schroder, T. B.; Starr, F. W.; Glotzer, S. C. *Phys. Rev. E* **2001**, 6405.
(53) Donati, C.; Douglas, J. F.; Kob, W.; Plimpton, S. J.; Poole, P. H.; Glotzer, S. C. *Phys. Rev. Lett.* **1998**, *80*, 2338.
(54) Kob, W.; Donati, C.; Plimpton, S. J.; Poole, P. H.; Glotzer, S. C. *Phys. Rev. Lett.* **1997**, *79*, 2827.
(55) Vogel, M.; Doliwa, B.; Heuer, A.; Glotzer, S. C. *J. Chem. Phys.* **2004**, *120*, 4404.